THE JOURNAL OF PHYSICAL CHEMISTRY A

 VOLUME 104, NUMBER 27, JULY 13, 2000

ARTICLES

Time-Resolved Photodissociation (TRPD) of the Naphthalene and Azulene Cations in an Ion Trap/Reflectron

Weidong Cui, Boaz Hadas, Baopeng Cao, and Chava Lifshitz*

Department for Physical Chemistry and The Farkas Center for Light Induced Processes, The Hebrew University of Jerusalem, Jerusalem 91904, Israel

Received: February 2, 2000; In Final Form: April 21, 2000

Dissociation rates have been measured by multiphoton ionization and time-resolved photodissociation for benzene-$d_6^{\bullet+}$, naphthalene-$h_8^{\bullet+}$, naphthalene-$d_8^{\bullet+}$, and azulene-$h_8^{\bullet+}$ employing a quadrupole ion trap/reflectron mass spectrometer. Results compare favorably with available data from ICR cells and cylindrical ion traps. Azulene$^{\bullet+}$ is photodissociated upon absorption of two 400 nm photons giving C_2H_2, H$^{\cdot}$, and H_2 eliminations. Dissociation rate constants measured for naphthalene$^{\bullet+}$ and azulene$^{\bullet+}$ at identical absolute energies are equal within experimental error. This experimental result is in agreement with previous density functional theory (DFT) calculations that demonstrated the isomerization of azulene$^{\bullet+}$ to naphthalene$^{\bullet+}$ below the dissociation limit of benzocyclobutadiene$^{\bullet+}$ + acetylene.

Introduction

The competition between isomerization and dissociation of polyatomic cation radicals is a topic of great interest. It has been studied in great detail for various relatively small hydrocarbon isomers such as $C_4H_6^{\bullet+}$ and $C_5H_{10}^{\bullet+}$ by Baer and coworkers using photoelectron photoion coincidence (PEPICO),[1−3] but not for larger hydrocarbons such as polycyclic aromatic hydrocarbon (PAH) isomers. The mass spectral fragmentation patterns obtained for different PAH isomers are nearly identical, suggesting extensive isomerization of many of the parent ions prior to dissociation.[4] PAHs and their cations have been proposed as carriers of the unidentified emission bands observed from the interstellar medium.[5−7] This has led to considerable work concerning their photoionization and photofragmentation. Photoionization in the VUV, combined with mass spectrometry, has been applied to naphthalene[8,9] and azulene.[8] The two major reaction channels of naphthalene$^{\bullet+}$ and azulene$^{\bullet+}$ are C−H bond cleavage and acetylene elimination. The acetylene loss reaction was studied in naphthalene by threshold photoelectron photoion coincidence (T-PEPICO).[10] Both channels were studied in naphthalene by time-resolved photodissociation (TRPD).[11] Microcanonical rate−energy, $k(E)$ curves were determined and modeled using RRKM theory.[11] A recent photodissociation study of PAH cations[12] has found naphthalene$^{\bullet+}$ to be photodestroyed whereas azulene$^{\bullet+}$ was determined to be photostable.

The naphthalene/azulene monocation isomerization has come under scrutiny recently[13] through density functional and coupled cluster calculations. The transition state barrier energies for isomerization were found to be lower by ≥ 13 kcal/mol than the dissociation limit of $C_8H_6^{\bullet+}$ + C_2H_2. The structure of the acetylene elimination product ion from naphthalene$^{\bullet+}$ was demonstrated by calculations[14,15] and through charge reversal experiments[16] to be benzocyclobutadiene$^{\bullet+}$. Acetylene elimination from azulene$^{\bullet+}$ was demonstrated[16] to lead to the same (benzocyclobutadiene$^{\bullet+}$) product ion. The most advanced experiments[16] and computations[13] thus point to isomerization of azulene$^{\bullet+}$ to naphthalene$^{\bullet+}$ below the dissociation limit for acetylene elimination.

10.1021/jp000419b CCC: $19.00
Published on Web 06/16/2000

Isomeric ions, whose isomerization barrier is lower than the dissociation limit and that can rapidly isomerize to the lowest energy isomer prior to dissociation, undergo dissociation with identical rate constants.[17] This type of experimental test for isomerizing ions has been applied to the anthracene/phenanthrene cation radical pair using time-resolved photoionization mass spectrometry (TPIMS) and RRKM modeling.[18] Microcanonical rate energy dependences $k(E)$ deduced for H loss and C_2H_2 loss were plotted as a function of the absolute energy. The two sets of $k(E)$ curves, for anthracene and phenanthrene respectively, did not coalesce into one, as they should have in the case of a fast isomerization.

The determination of $k(E)$ via TRPD is much more direct and accurate than by time-resolved photoionization and is the subject of this presentation. Refined time and energy resolved data for the naphthalene cation were obtained jointly by TPIMS and TRPD.[11] TRPD is particularly well suited for energy resolved measurements of slow dissociation processes.[19−25] Traditionally, TRPD, which has been developed by Dunbar and co-workers, has employed the FTICR technique for ion trapping and mass spectrometric measurements. In TRPD, ions are produced by an electron ionization pulse or by a laser multiphoton ionization (MPI) pulse. They are allowed to relax to their ground state for a preselected time, then they are photoexcited by a short laser pulse, after which follows the time resolved appearance curve of a mass selected product ion. This can be done for different photon energies provided the ions absorb in the right wavelength region. Microcanonical rate constants are deduced by this method for time ranges that are impossible to achieve by PEPICO, namely in the millisecond range.

The FTICR is not a necessary prerequisite for TRPD measurements, and simpler ion trapping devices may suffice. Neusser and co-workers[25] succeeded in measuring the unimolecular decay of perdeuterated benzene$^{\bullet+}$ with a cylindrical ion trap (CIT), the simplest version of an ion trap. The suitability of our instrumentation, a quadrupole ion trap/reflectron device, for decay time investigations will be demonstrated first through repeating the previously published single-laser, one-color photodissociation of perdeuterated benzene.[25] This will be followed by a two-color, two-laser photodissociation experiment on naphthalene to be compared with the previous TRPD results from FTICR experiments.[11] It will be demonstrated that the results from the quadrupole ion trap are in good agreement with the literature data.

We have chosen for the test concerning isomerization the simplest pair of PAH isomers for which we have carried out the ab initio computations:[13] naphthalene$^{\bullet+}$ and azulene$^{\bullet+}$. We will present microcanonical $k(E)$ data on this pair of isomers, derived using TRPD on the quadrupole ion trap/reflectron device.

Experimental Section

The experimental apparatus and some of the methods employed have been described by us in detail previously.[26−28] The instrument (Figure 1) consists of a reflectron time-of-flight mass spectrometer with a quadrupole ion trap as an ion source (from R. M. Jordan Company). It has been developed originally by Lubman and co-workers[29] to combine the storage capabilities of an ion trap with the speed and resolution of a time-of-flight device. The goal of our research employing such a combination is similar to that of Neusser's, namely the observation of unimolecular decay of energy selected ions on the ms time scale combined with a fast mass detection process.[30] We have upgraded the instrument we have employed previously[26−28] by using two Continuum laser systems, each combining a ND6000 dye laser pumped by a Nd:YAG Surelite laser. One of the lasers was used for photoionization and the other for photodissociation of the parent ion. The cations are currently produced in an effusive molecular beam with thermal temperatures. A brief description of the apparatus follows. The quadrupole ion trap (a "Paul-trap"[31]) consists of two endcap electrodes and a ring electrode situated between the two endcaps. By placing ceramic spacers between these three electrodes the ion trap is completely enclosed. The inside surfaces of the trap are hyperbolic. There are six 3.5 mm diameter apertures. Two apertures are in the two endcaps, one of which was used for ion ejection. Four are in the ring electrode with two at the top and bottom (vertical direction), the top one being used as the neutral sample inlet, and the other two are in the horizontal direction for the laser beams. During operation, the RF voltage is applied to the ring electrode while both endcaps are held at 0 V. The RF field serves to trap ions present within the volume of the trap until they are ejected by application of a DC extraction pulse to the exit endcap. A digital delay generator triggered by the laser Q-switch output controls the storage time of the ions. The digital delay generator triggers the extraction pulser which serves the dual purpose of ejecting the ions and providing the start-time reference for the TOF mass analysis by triggering the model LeCroy 9450A digital oscilloscope. The reflectron apparatus was operated under the energy correction mode for unit mass resolution.

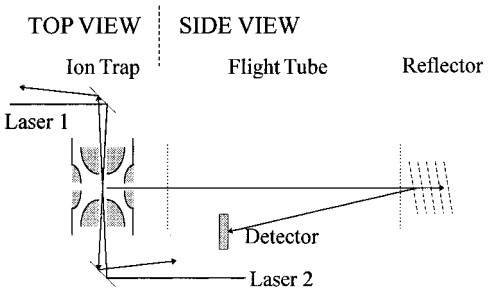

Figure 1. Quadrupole ion trap/reflectron time-of-flight mass spectrometer. In time-resolved photodissociation, laser no. 1 causes ionization and laser no. 2 causes dissociation.

All of the neutral samples, including benzene-d_6, naphthalene-h_8, naphthalene-d_8, and Azulene-h_8, were from Sigma−Aldrich at the highest purity available and were introduced into the ion source by a leak valve.

The experiment using C_6D_6 follows that of Grebner and Neusser.[25] Ionization and excitation of the benzene ion were performed with three photons of the same color at 265 nm, the frequency-doubled output of the dye laser (Coumarin 500) pumped by a 10 ns pulse Nd:YAG laser (10 Hz). The first and second absorbed photon excites and ionizes the perdeutero benzene via the 6_1^0 hot band transition. The absorption of the third photon in the cation leads to an ion internal energy of 4.67 eV. Mass spectrometric measurements were carried out following variable trapping times.

Naphthalene-h_8, naphthalene-d_8, and azulene-h_8 underwent two-color ionization and excitation. The ionization and excitation laser beams passed through the ion trap from opposite directions with maximum overlap at the center (see Figure 1). In the two-color experiments, a four-channel digital delay/pulse generator (Stanford Research Systems, Inc.) controlled the delay between the two lasers. Figure 2 shows the timing sequence employed in the measurements. The neutral molecules were ionized by absorption of two photons of the first laser (253 nm from the

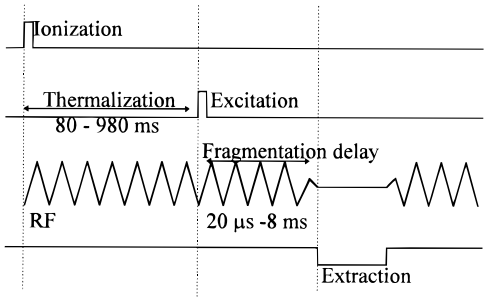

Figure 2. Pulse sequence for theTRPD experiment.

TABLE 1: Experimental Parameters[a]

sample	pressure[b] (10^{-6} Torr)	ionization laser (power)	excitation laser (power)
benzene-d_6	1.8	265 nm (0.4 mJ)	
naphthalene-h_8	4.0	253 nm (0.02mJ)	355 nm (1.6−1.7mJ)
naphthalene-d_8	4.2	253 nm (0.03 mJ)	355 nm (1.6−1.7 mJ)
azulene-h_8	3.4	317.5 nm (0.03 mJ)	400 nm (1.5−1.6 mJ)

[a] All the laser beams were focused. [b] These are nominal pressures measured on an ionization gauge situated outside the ion trap.

mixing after doubling and 317.5 nm from the doubled output of DCM for naphthalene and azulene, respectively). The working frequency for the delay/pulse generator was selected according to the desired thermalization time, e.g., 10 Hz for an 80 ms thermalization time, 1 Hz for 980 ms, etc. The four-channel output pulses were applied to the two Nd: YAG lasers pumping the two dye lasers, with two pulses for the flash lamps and two for the Q-switches, respectively. One pulse to the flash lamp of the ionization laser system was synchronized with the RF pulse, so that the sample ions produced by the first laser could be trapped for thermalization by collisional and radiative cooling at room temperature. The thermalization time was the delay between the two pulses applied to the Q-switches. After thermalization, the ions were irradiated by the second laser for excitation (at 355 nm, the third harmonic of the Nd:YAG laser for the naphthalene ion, and at 400 nm, the mixing output of DCM for the azulene ion). Time-resolved dissociation processes could be recorded following the excitation pulse. In the two-laser experiments, care was taken to suppress the daughter ion signals caused by multiphoton ionization to zero by adjusting the ionization laser intensity, which was kept constant in all of the measurements. Dissociation resulted solely by the excitation laser. Time-dependent daughter ion intensities were normalized via the corresponding parent ion intensities, taking the parent intensity at the shortest trapping time as the reference point, to take into account fluctuations in light intensity for different laser shots.

Pressures were measured by an ionization gauge outside the ion-trapping device, without correction by the gauge calibration factor. The experimental parameters employed are summarized in Table 1.

III. Results and Discussion

1. Comparison with Previous Results. *(a) One-Color Photoionization and Time-Resolved Photodissociation of C_6D_6.* In the Grebner and Neusser CIT experiment[25] the ionization of C_6D_6 and excitation of the $C_6D_6^{\bullet+}$ cation were performed with three photons at 37723 cm^{-1}, which led to an ion internal energy of 4.67 eV. In our experiment, the ions were generated at the same internal energy level and the buildup of the D-loss product, $C_6D_5^+$, was measured from 50 μs to 4.5 ms trapping time with a 50 μs stepwise increase at the early stages. By fitting the rise

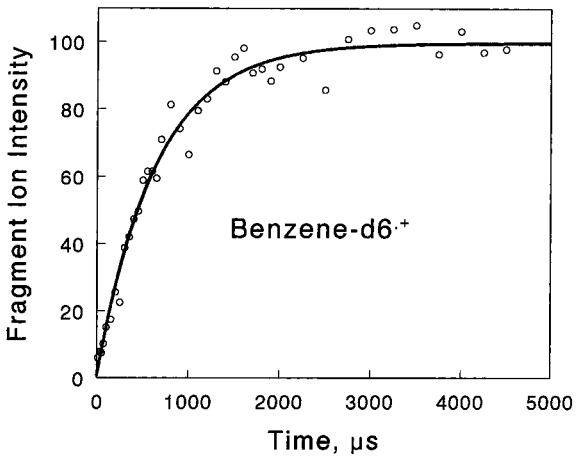

Figure 3. Signal of $C_6D_5^+$ from the reaction $C_6D_6^{\bullet+} \rightarrow C_6D_5^+ + D^{\bullet}$ in benzene-d_6 with increasing trapping time after one-color three-photon ionization and excitation described in the text. The experimental points are fitted with a single-exponential curve (solid line) yielding an inverse time constant $1.55 \pm 0.1 \times 10^3$ s^{-1} for an ion internal energy, $E_{ion} = 4.67$ eV.

of the measured $C_6D_5^+$ intensity with increasing trapping time using a single exponential buildup function, a rate constant of $1.55 \pm 0.1 \times 10^3$ s^{-1} (inverse time constant) was obtained, which is in good agreement with the previous result[25] 1.5×10^3 s^{-1} (Figure 3). The previous result was based not only on an effusive beam experiment but also on a supersonic expansion experiment at very low background pressures.[25] The agreement obtained between the present value and the previous result is gratifying since it indicates that collisional relaxation does not perturb our determination of the apparent dissociation time constant.

(b) Two-Color Photoionization and Time-Resolved Photodissociation of Naphthalene and Deuterated Naphthalene. In the Ho, Dunbar, and Lifshitz FTICR experiment,[11] neutral naphthalene was ionized by MPI at 193 nm and the sample pressure was on the order of 10^{-8} Torr. The ions were thoroughly thermalized at 300 K by collisional and radiative cooling during a minimum delay of 4 s before applying the excitation pulse. In the present work, naphthalene was ionized by 253 nm photons. Excitation of the naphthalene ion was by two photons at 355 nm, leading to an internal energy of 7.1 eV as in the former experiment.[11] Collisional thermalization prior to excitation of the ions produced was expected to be faster in the present experiment, in view of the much higher sample pressures employed ($\geq 10^{-6}$ Torr). The first experiments were aimed at choosing the optimum thermalization time.

Experiments for naphthalene were done at three relaxation times: 180, 480, and 980 ms. The rise of the acetylene loss product ion was measured as a function of increasing trapping time from 20 μs to 8 ms. The time-resolved appearance curves showed apparently exponential time dependence. The TRPD curve for a thermal ion population deviates in general from exponential decay, but the deviation is very slight if the thermal internal energy is small compared with the internal energy of the photoexcited ion. The rate constants (inverse time constants) derived from fitting by single exponential functions were found to be decreasing with increasing relaxation time (Table 2). Although we should be cautious in implying that the results presented in Table 2 refer to fully relaxed thermal ions, the agreement of the lowest dissociation rate with the literature value lends support to this assumption. The rate constant 6400 s^{-1} obtained at a 980 ms relaxation time is close to the literature

TABLE 2: Dissociation Rate Constants for TRPD of Naphthalene Ions at 355 nm after Different Thermalization Times

thermalization time	total dissociation rate (s^{-1})[a]
180 ms	11800 ± 1700
480 ms	9370 ± 1500
980 ms	6400 ± 1500

[a] Measured inverse time constants; each value is an average of at least three separate measurements.

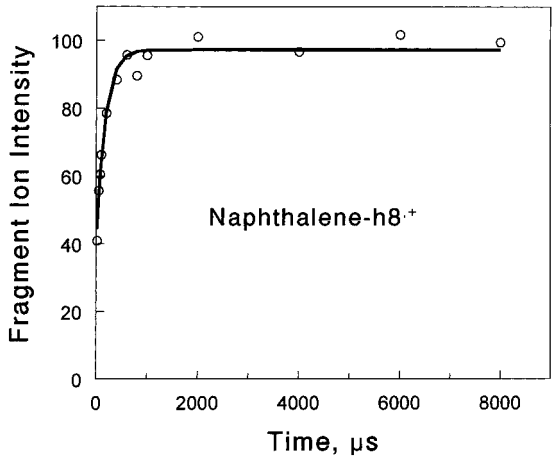

Figure 4. TRPD points for dissociation of $C_{10}H_8^{\bullet+}$ from naphthalene by two photons at 355 nm corresponding, upon inclusion of the average thermal energy, to an ion internal energy $E_{ion} = 7.1$ eV. The points are the relative signal intensities of the $C_8H_6^{\bullet+}$ fragment peak. The solid curve is a single-exponential fit, yielding an inverse time constant 6.4 ± 1.5 s^{-1}.

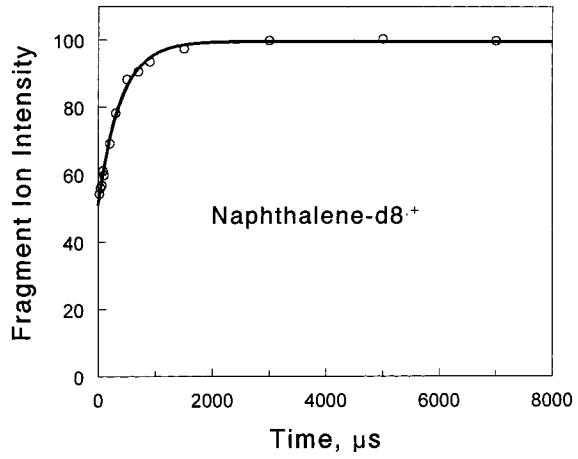

Figure 5. TRPD curve, similar to Figure 4, for dissociation of $C_{10}D_8^{\bullet+}$ from naphthalene-d_8. The fitted exponential curve yields an inverse time constant 2.40 ± 0.19 s^{-1}.

value[11] of 6450 s^{-1}, and 980 ms was chosen as the preferred relaxation time.

All of the conditions were kept the same for deuterated naphthalene, and a rate constant of 2410 ± 190 s^{-1} was obtained, which is also in good agreement with the literature value[11] of 2360 s^{-1}. Figures 4 and 5 show typical TRPD curves for the naphthalene-h_8/naphthalene-d_8 pair.

2. Time-Resolved Photodissociation of the Azulene Cation. As noted in the Introduction, it is well known from the work of Baer and co-workers[1−3,17] that dissociation rates of isomeric ions are identical at similar absolute energies if they rearrange to a common precursor ion prior to dissociation. The constituent elements of the naphthalene$^{\bullet+}$/azulene$^{\bullet+}$ isomer pair, 10 carbon atoms and four hydrogen molecules in their standard states at 0 K, are taken as the zero of the absolute energy scale. In the experiment described in section 1(b) above, naphthalene ions were excited to an internal energy level of 7.1 eV by absorption of two 355 nm photons. The corresponding absolute energy is calculated to be 17.04 eV by adding 7.1 eV to the 0 K heat of formation of the naphthalene ion,[9] $\Delta H_f^\circ{}_0$ (naphthalene$^{\bullet+}$) = 229.2 kcal/mol. Azulene ions were generated by absorption of two photons at 317.5 nm followed by a thermalization delay time and a 400 nm-laser excitation pulse. The heat of formation of the azulene cation, $\Delta H_f^\circ{}_0$ (azulene$^{\bullet+}$) = 247 kcal/mol, is higher than that of the naphthalene cation by 17.8 kcal/mol,[13] and the average thermal energy is 0.13 eV. If two 400 nm photons are absorbed by the azulene ion in the TRPD experiment, the absolute energy is calculated to be 17.04 eV, which exactly matches the absolute energy in the naphthalene experiment.

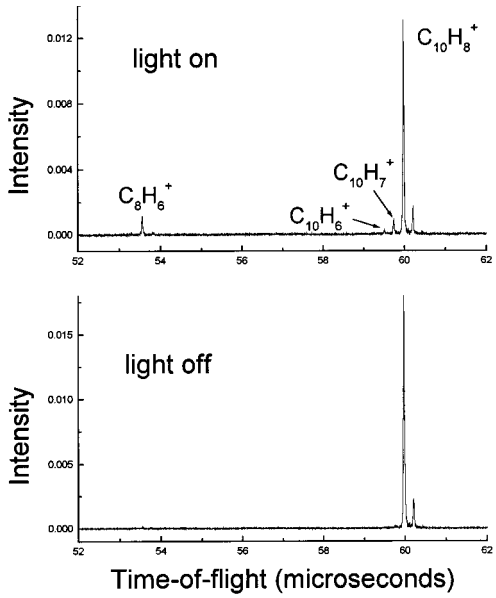

Figure 6. Photodissociation mass spectra for dissociation of azulene$^{\bullet+}$ by two-photon dissociation at 400 nm.

Figure 6 illustrates the photodissociation mass spectrum of azulene, showing that the fragment ions $C_{10}H_7^+$, $C_{10}H_6^{\bullet+}$, and $C_8H_6^{\bullet+}$ are all formed in observable abundance as in the case for naphthalene.[11] The azulene radical cation is observed to undergo laser photodissociation at 400 nm. Using a xenon arc lamp with a radiation flux of 10^{17} photons s^{-1} cm^{-2} nm^{-1} and a smooth spectral profile resembling a 6200 K blackbody, azulene$^{\bullet+}$ was observed to be essentially photostable.[12] In the present laser experiment, the average energy employed, 1.5 mJ per pulse, i.e., 1.5 mJ per 10 ns, corresponds to a radiation flux several orders of magnitude higher than that of the xenon arc experiment and specifically at 400 nm. The absorption spectrum of azulene$^{\bullet+}$ is not known and may be quite different from that of naphthalene$^{\bullet+}$. This explains the discrepancy between the two experiments. Jochims et al.[8] have proposed a scheme to account for the photofragmentation of the azulene$^{\bullet+}$ and naphthalene$^{\bullet+}$ isomers. They concluded that the isomers are linked by a common intermediate from which hydrogen and acetylene loss occurs. Ekern et al.[12] discarded this scheme because azulene$^{\bullet+}$ was found to be photostable and naphthalene$^{\bullet+}$ was observed to be photodissociated. The present laser photodissociation experiments are entirely in accord with this scheme. In fact, the branching ratios between H$^\cdot$ and C_2H_2 losses from azulene$^{\bullet+}$ (Figure 6) are very nearly the same as for naphthalene$^{\bullet+}$ at the same absolute energy.[11]

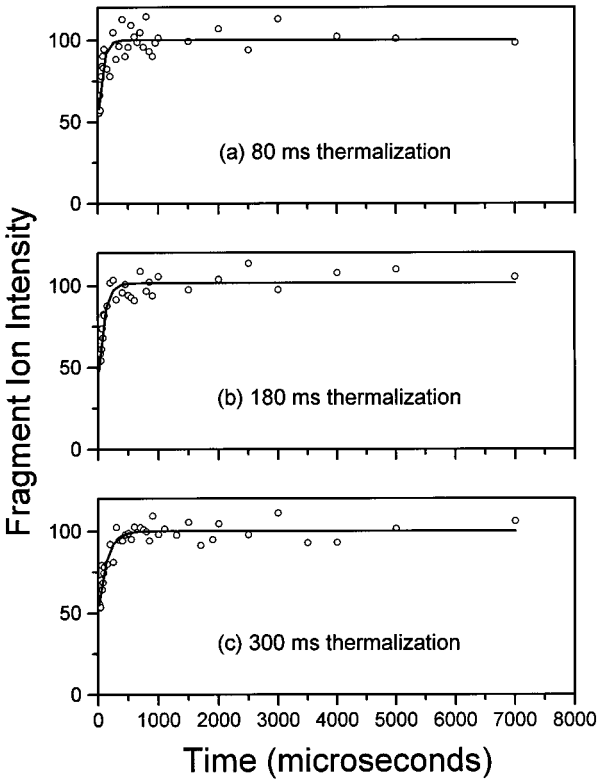

Figure 7. TRPD points for dissociation of $C_{10}H_8^{\bullet+}$ from azulene by two photons at 400 nm. The points are the relative signal intensities of the $C_8H_6^{\bullet+}$ fragment peak after the indicated thermalization times. The curves are single-exponential fits leading to decreasing inverse time constants with increasing thermalization (see text).

TABLE 3: Dissociation Rate Constants for TRPD of Azulene Ions at 400 nm after Different Thermalization Times

thermalization time	total dissociation rate (s^{-1})[a]
80 ms	14700 ± 3700
180 ms	8450 ± 2400
300 ms	7260 ± 1700

[a] Measured inverse time constants; each value is an average of at least three separate measurements.

Time-resolved appearance curves at 400 nm showed apparently exponential time dependence. The rise of the acetylene loss product with increasing trapping time was measured, and inverse time constants were obtained by single-exponential function fitting (Figure 7). The time constants obtained for different thermalization times are summarized in Table 3.

The results presented in Table 3 demonstrate that the fitted inverse time constants decrease with increasing thermalization time. We could not measure one additional appearance curve of the daughter ion, at a thermalization time much longer than 300ms, because of the decrease of the light intensity at 400 nm upon reduction of the working frequency of the delay/pulse generator. Following ionization by two 317.5 nm photons, the azulene ion has an excess energy of only 0.4 eV. As a result, it needs shorter time for thorough thermalization than the naphthalene ion that is formed with an excess energy of 1.66 eV. The available rate constants for azulene$^{\bullet+}$ (Table 3) are seen to begin to level off already after a thermalization time of 180 ms and to approach the naphthalene$^{\bullet+}$ 6450 s^{-1} value (within fairly large error limits). This indicates that isomerization between the two cations does take place below the dissociation limit, in agreement with our recent computational results.[13] A schematic potential energy profile for the isomerization of naphthalene$^{\bullet+}$ and azulene$^{\bullet+}$, and for dissociation via acetylene elimination, based on our recent density functional theory (DFT) and coupled cluster calculations[13,15] and on the present experiments is presented in Figure 8. In this figure, the intermediates calculated for the Dewar−Becker isomerization mechanism,[13] including the key hydrogen-shifted naphthalene$^{\bullet+}$ isomer, have been omitted and only the highest barrier along the isomerization path, a transition state corresponding to the norcaradiene$^{\bullet+}$ isomer, is included.

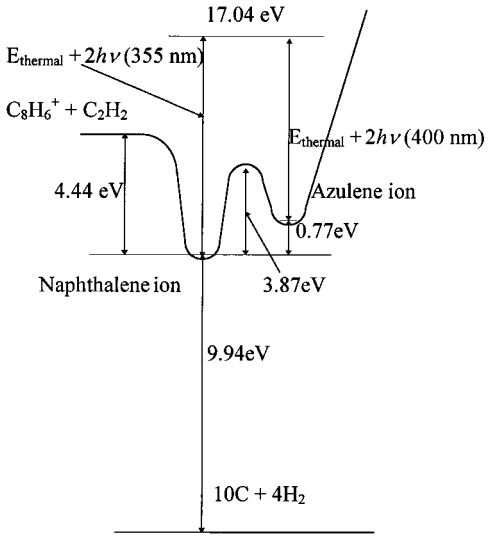

Figure 8. Schematic potential energy profile for the isomerization and dissociation of the naphthalene$^{\bullet+}$/azulene$^{\bullet+}$ isomer pair.

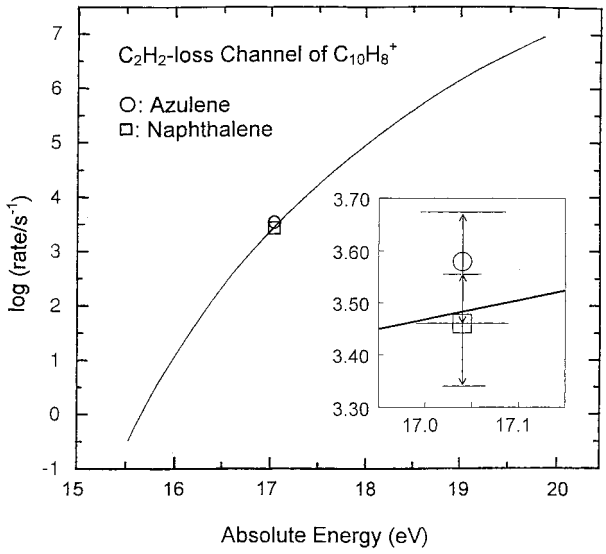

Figure 9. TRPD experimental values for the rate constants for acetylene loss from naphthalene$^{\bullet+}$(□) and azulene$^{\bullet+}$(○). The curve is the RRKM rate−energy curve corresponding to the naphthalene$^{\bullet+}$ model from ref 11 plotted as a function of absolute energy.

The rate−energy curve for the acetylene loss channel, calculated previously as a function of internal energy of the naphthalene ion by RRKM/QET,[11] was calculated and replotted as a function of the absolute energy (Figure 9). The two experimental TRPD points for naphthalene$^{\bullet+}$ and azulene$^{\bullet+}$ obtained in the present work are marked on the curve. It should be noted that this curve is for the acetylene loss channel. The TRPD experiments give the total dissociation rate constants of the parent ions. The rate constant for acetylene loss is calculated from the minimum total inverse time constant and from the branching

ratio for acetylene loss, taking into account the branching ratios of all the daughter ions in the TRPD experiment.

The $k(E)$ point for azulene$^{\bullet+}$ (Figure 9) falls on the naphthalene$^{\bullet+}$ curve within error limits. If it were possible to measure one more point at longer thermalization time for azulene$^{\bullet+}$, the overlap might have improved. This notwithstanding, the present work demonstrates that isomerization from azulene$^{\bullet+}$ to naphthalene$^{\bullet+}$ occurs, and the deep potential well of the naphthalene$^{\bullet+}$ cation radical is sampled leading, in azulene$^{\bullet+}$, to the same low rate constant as in naphthalene$^{\bullet+}$. In the case of pairs of isomers residing in a deep and shallow well, respectively, PEPICO experiments[1−3] find two rate constants, a slow one and a fast one, when the less stable isomer is initially produced. The slow rate, corresponding to the exit from the deep potential well, is the one that is equal for both isomers. Is there an additional fast rate in the case of azulene$^{\bullet+}$ that is not present for naphthalene$^{\bullet+}$? If that were the case, then it would be outside the time range of our measurements. There is a finite dissociation at zero delay time, indicating a fast decay component (Figure 7). There are, however, similar finite intercepts also in the case of naphthalene-$h_8{}^{\bullet+}$ and naphthalene-$d_8{}^{\bullet+}$ (Figures 4 and 5, respectively). These are assigned to three-photon excitation processes that lead to fast dissociations. The dissociation of azulene$^{\bullet+}$ through acetylene elimination can most probably not circumvent the deep well, since the $C_8H_6{}^{\bullet+}$ dissociation product, benzocyclobutadiene$^{\bullet+}$,[14−16] is produced via naphthalene$^{\bullet+}$. There is no direct dissociation due to acetylene elimination from azulene$^{\bullet+}$ competing with isomerization to naphthalene$^{\bullet+}$. As a result only one rate, the slow one, is to be expected. Direct dissociations of the $C_{10}H_8{}^{\bullet+}$ isomers due to C−H bond cleavages cannot be excluded, since the branching ratio for H_2 elimination is a factor ∼2.5 lower in azulene$^{\bullet+}$ than in naphthalene$^{\bullet+}$. We have not yet attempted a more complete study of all three reaction channels at a series of absolute energies.

3. Conclusions

The TRPD method has been employed for the first time using a quadrupole ion trap/reflectron TOF mass spectrometer. Microcanonical rate constants were obtained for benzene$^{\bullet+}$ and naphthalene$^{\bullet+}$ cation dissociations using single-color and two-color ionization and excitation schemes, respectively. The results are in good agreement with literature values. This demonstrates that a quadrupole ion trap is suitable for decay time investigations on the millisecond time scale, as are the ICR cell and the CIT. Azulene$^{\bullet+}$ is photodissociated at 400 nm, leading to acetylene, H$^{\bullet}$, and H_2 elimination products. Azulene$^{\bullet+}$ has the same inverse time constant for dissociation as naphthalene$^{\bullet+}$ when excited to the same absolute energy, in agreement with its undergoing isomerization to naphthalene$^{\bullet+}$ prior to acetylene loss.

Acknowledgment. This research was supported by The Israel Science Foundation founded by the Israel Academy of Sciences and Humanities and by The James Franck Foundation. The Farkas Research Center is supported by the Minerva Gesellschaft für die Forschung GmbH, München.

References and Notes

(1) Baer, T.; Hase, W. L. *Unimolecular Reaction Dynamics: Theory and Experiments;* Oxford: New York, 1996.

(2) Duffy, L. M.; Keister, J. W.; Baer, T. *J. Phys. Chem.* **1995**, *99*, 17862.

(3) Keister, J. W.; Baer, T.; Evans, M.; Ng, C. Y.; Hsu, C.-W. *J. Phys. Chem. A* **1997**, *101*, 1997.

(4) Pachuta, S. J.; Kenttämaa, H. I.; Sack, T. M.; Cerny, R. L.; Tomer, K. B.; Gross, M. L.; Pachuta, R. R.; Cooks, R. G. *J. Am. Chem. Soc.* **1988**, *110*, 657.

(5) Léger, A.; Puget, J. L. *Astron. Astrophys.* **1984**, *137*, L 5.

(6) Allamandola, L. J.; Tielens, A. G. G. M.; Barker, J. R. *Astrophys. J.* **1985**, *290*, L25.

(7) Salama, F.; Allamandola, J. L. *Astrophys. J.* **1992**, *395*, 301.

(8) Jochims, H. W.; Rasekh, H.; Rühl, E.; Baumgärtel, H.; Leach, S. *Chem. Phys.* **1992**, *168*, 159.

(9) Gotkis, Y.; Oleinikova, M.; Naor, M.; Lifshitz, C. *J. Phys. Chem.* **1993**, *97*, 12282.

(10) Rühl, E.; Price, S. D.; Leach, S. *J. Phys. Chem.* **1989**, *93*, 6312.

(11) Ho, Y.-P.; Dunbar, R. C.; Lifshitz, C. **1995**, *117*, 6504.

(12) Ekern, S. P.; Marshall, A. G.; Szczepanski, J.; Vala, M. *J. Phys. Chem. A* **1998**, *102*, 3498.

(13) Koster, G.; Lifshitz, C.; Martin, J. M. L. *J. Chem. Soc., Perkin Trans. 2* **1999**, *11*, 2383.

(14) Granucci, G.; Ellinger, Y.; Boissel, P. *Chem. Phys.* **1995**, *191*, 165.

(15) Ling, Y.; Martin, J. M. L.; Lifshitz, C. *J. Phys. Chem. A* **1997**, *101*, 219.

(16) Schroeter, K.; Schröder, D.; Schwarz, H. *J. Phys. Chem. A* **1999**, *103*, 4174.

(17) Werner, A. S.; Baer, T. *J. Chem. Phys.* **1975**, *62*, 2900.

(18) Ling, Y.; Lifshitz, C. *J. Phys. Chem. A* **1998**, *102*, 708.

(19) Dunbar, R. C. *J. Phys. Chem.* **1987**, *91*, 2801. So, H. Y.; Dunbar, R. C. *J. Am. Chem. Soc.* **1988**, *110*, 3080.

(20) Dunbar, R. C. *J. Phys. Chem*. **1990**, *94*, 3283. Huang, F. S.; Dunbar, R. C. *J. Am. Chem. Soc*. **1990**, *112*, 8167.

(21) Faulk, J. D.; Dunbar, R. C. *J. Am. Chem. Soc*. **1992**, *114*, 8596.

(22) Gotkis, Y.; Naor, M.; Laskin, J.; Lifshitz, C.; Faulk, J. D.; Dunbar, R. C. *J. Am. Chem. Soc*. **1990**, *112*, 8167. Dunbar, R. C.; Lifshitz, C. *J. Chem. Phys.* **1991**, *94*, 3542.

(23) Klippenstein, S. J.; Faulk, J. D.; Dunbar, R. C. *J. Chem. Phys*. **1993**, *98*, 243.

(24) Ho, Y.-P.; Dunbar, R. C. *J. Phys. Chem*. **1993**, *97*, 11474. Lin, C. Y.; Dunbar, R. C. *J. Phys. Chem*. **1994**, *98*, 1369.

(25) Walther, C.; Dietrich, G.; Lindinger, M.; Lützenkirchen, K.; Schweikhard, L.; Ziegler, J. *Chem. Phys. Lett.* **1996**, *256*, 77. Lindinger, M.; Dasgupta, K.; Dietrich, G.; Krückeberg, S.; Kuznetsov, S.; Lützenkirchen, K.; Schweikhard, L.; Walther, C.; Ziegler, J. *Z. Phys. D* **1997**, *40*, 347.

(26) Grebner, Th. L.; Neusser, H. J. *Int. J. Mass Spectrom*. **1999**, *185/186/187*, 517.

(27) Weickhardt, C.; Lifshitz, C. *Eur. Mass Spectrom*. **1995**, *1*, 223.

(28) Laskin, J.; Lifshitz, C. *Chem. Phys. Lett*. **1997**, *277*, 564.

(29) Laskin, J.; Hadas, B.; Märk, T. D.; Lifshitz, C. *Int. J. Mass Spectrom.* **1998**, *177*, L9.

(30) Michael, S. M.; Chien, B. M.; Lubman, D. M. *Rev. Sci. Instrum.* **1992**, *63*, 4277.

(31) Grebner, Th. L.; Neusser, H. J. *Int. J. Mass Spectrom.* **1994**, *137*, L1.

(32) Paul, W. *Angew. Chem., Int. Ed. Engl.* **1990**, *29*, 739.